

Pion Cloud and Nucleon Mass in Finite Nuclei

Andrew J. Harey* and Leonard S. Kisslinger†

Department of Physics, Carnegie Mellon University, Pittsburgh, Pennsylvania 15213-3890

(November 9, 2018)

We study the mass of a nucleon in a nucleus using a model recently introduced for a nucleon current with a pion cloud component. The method of QCD sum rules is used to determine the mass shifts for nucleons to first order in nuclear density in ^{16}O and ^{40}Ca , with the pion propagator determined by an optical potential for pion-nucleus scattering. Mass shifts due to the pionic contributions range from negligible in oxygen to -100 MeV in calcium at central nuclear density, with larger shifts in the nuclear surface. The consistency of this model with chiral perturbation theory is demonstrated.

11.30.Rd,11.55.Hx,12.38.Lg,13.75.Gx,14.20.Dh,21.10.Dr,21.65.+f,24.85.+p

arXiv:nucl-th/0005005v1 1 May 2000

*E-mail:harey@cmu.edu

†E-mail:kissling@andrew.cmu.edu

I. INTRODUCTION

Until the pioneering work of Drukarev and Levin on the use of QCD sum rules in systems of finite nucleon density [1], descriptions of nucleons in nuclear matter had mostly been based on models of N - N interactions [2] or the direct use of meson exchange potentials in quantum hadrodynamics [3]. These models have serious problems at both the short-distance and long-distance scales. At short distance one must treat the complex structure of hadrons, for which we now believe that QCD gives the correct description. At long-distance scales it seems that meson cloud effects must be included, and neither quantum hadrodynamics nor current treatments of QCD are adequate; while chiral perturbation theory [4,5] is very successful in a quantitative treatment of pionic effects at low energies. Recently a model was developed for use in QCD sum rules with a nucleon current that has a Goldstone boson component, which has the main features of both microscopic QCD and chiral perturbation theory [6]. In the present paper we extend this model for the study of nucleons in finite nuclei.

The strongest experimental evidence for the utility of introducing an explicit meson cloud component for the nucleon is the data on sea quark distributions obtained from Drell-Yan experiments. The NMC/CERN experiments [7] have given evidence for violation of the Gottfried sum rule

$$\int_0^1 \frac{dx}{x} [F_2^p(x) - F_2^n(x)] = \frac{1}{3} \int_0^1 \{ [u_p^v(x) - d_p^v(x)] + 2 [\bar{u}_p^v(x) - \bar{d}_p^v(x)] \} dx. \quad (1.1)$$

If the up-type and down-type sea quark distributions are equal, as would be expected from QCD, then the value of this integral is $1/3$. The NMC result is 0.24 ± 0.016 at $Q^2 = 5 \text{ GeV}^2$ over the interval $0.004 \leq x \leq 0.8$. Similar effects were found in Drell-Yan measurements from Fermilab/E866 [8], where the ratio of down to up sea quark distributions is much larger than 1.0. Both of these results differ from the predictions of perturbative [9] and nonperturbative [10] QCD calculations. One approach to account for this discrepancy in sea quark distributions in hadronic models is to include a meson cloud for the nucleon [11–13]. Our approach is to treat the pion as a basic Goldstone boson field at low energy, along with quarks and gluons, with separation of long-distance from medium- and short-distance effects.

Another strong motivation for introducing a correlator with a Goldstone boson component for use in QCD sum rules is given by chiral perturbation theory. It was shown almost two decades ago [14] that the leading nonanalytic contribution (LNAC) to the nucleon mass in chiral perturbation theory is a m_π^3 correction, with the lowest-order chiral logs not contributing. In the standard formulation of QCD sum rules one does not obtain such a m_π^3 term [15]. In Ref [6] it was shown not only that one obtains the m_π^3 LNAC, but that the known value of the mass shift (15 MeV) can be used to help determine the parameters of the model, in spite of the fact that the sum rule method is only accurate to about 10% for the nucleon mass. It is not possible to obtain the LNAC m_π^3 term with the usual quark fields correlator [15,6]. We make use of this result in the present work.

It should also be noted that in the QCD sum rule method the microscopic QCD calculation gives $m_\pi^2 \ln(m_\pi^2)$ terms for the nucleon in vacuum and also ρm_π terms for nucleons in the nuclear medium, both in contradiction to chiral perturbation theory. It was shown that both for the vacuum [15] and for nuclear matter [16] a careful treatment of the continuum part of the phenomenological correlator enables one to cancel these terms, which are inconsistent with chiral perturbation theory. We made use of this cancellation of unwanted logs in the formulation of our model [6] and use this mechanism in the present work.

We review Goldstone boson/QCD model of Ref. [6] for a nucleon in the vacuum in Section 2. In Section 3 the surface effects on the pion propagator are quantified using a p-wave πA optical potential where the $\Delta(1232)$ resonance is dominant. We extend the model for the microscopic correlator from zero to finite density in Section 4, with the goal of calculating nucleon mass shifts due to the pion cloud effects in small symmetric finite nuclei. The sum rules are then constructed and evaluated in the final sections.

II. REVIEW OF NUCLEON CORRELATOR WITH PION CLOUD IN VACUUM

In this section we review the model for the nucleon correlator with explicit Goldstone boson fields developed in Ref [6]. The nucleon current has the form

$$\eta^N(x) = c_1 \eta^{N,0}(x) + c_2 \eta^{N,\pi}(x) \quad (2.1)$$

where the constants c_i are the amplitudes of the composite field operator without and with the Goldstone boson field. This operator is used to construct the nucleon correlator. We ignore possible contributions to the nucleon from the strange part of the meson cloud. The proton field operator without the pion cloud is chosen to be the current [17]

$$\eta^{p,0}(x) = \epsilon^{abc} [u^a(x)^T C \gamma_\mu u^b(x)] \gamma_5 \gamma^\mu d_c(x), \quad (2.2)$$

where a, b, c label the color indices, and $u(x), d(x)$ are the up and down quark fields. C is the charge conjugation operator. The lowest-energy contribution to the phenomenological dispersion relation for the correlator, the pole term giving the proton intermediate state, depends on the transition matrix element

$$\langle 0 | \eta^{p,0}(p) | \text{proton} \rangle = \lambda_p v(p), \quad (2.3)$$

where λ_p is a structure constant and the Dirac spinor $v(p)$ is normalized by

$$\bar{v}(p)v(p) = 2m. \quad (2.4)$$

The neutron current $\eta^{n,0}(x)$ can be obtained by the interchange of up and down quark fields in Equation (2.2). The nucleon current including the explicit Goldstone boson field is taken to be

$$\eta^{p,\pi}(x) = \frac{1}{\lambda_\pi^2} \partial_\alpha \phi_\pi(x) \cdot \tau \gamma^\alpha \gamma^\beta \eta^{N,0}(x), \quad (2.5)$$

where $\phi_\pi(x)$ is a massless pion field, τ is the I-spin operator and λ_π is a $D = 1$ scale parameter. The structure constant of this current is defined by the relation

$$\langle 0 | \eta^{p,\pi}(x) | \text{proton} \rangle = \lambda'_p v(p). \quad (2.6)$$

The p-wave coupling of the pion to the nucleon current and experience with hybrid mesons [18] suggests that $\lambda_p'^2 \ll \lambda_p^2$, so we expect little contribution to the phenomenological expression for our nucleon correlator from the resulting pole due to its very small residue.

The full correlator for the proton with the pion cloud is

$$\begin{aligned} \Pi^p(p) &= i \int d^4x e^{ip \cdot x} \langle 0 | T [\eta^p(x) \bar{\eta}^p(0)] | 0 \rangle \\ &= c_1^2 i \int d^4x e^{ip \cdot x} \langle 0 | T [\eta^{p,0}(x) \bar{\eta}^{p,0}(0)] | 0 \rangle + (1 - c_1^2) i \int d^4x e^{ip \cdot x} \langle 0 | T [\eta^{p,\pi}(x) \bar{\eta}^{p,\pi}(0)] | 0 \rangle \\ &= c_1^2 \Pi^{(p,0)}(p) + (1 - c_1^2) \Pi^{(p,\pi)}(p). \end{aligned} \quad (2.7)$$

With the appropriate changes of current and isospin considerations, the neutron correlator is obtained. This model focuses on the long-range effects of the pion cloud and therefore does not include pion-quark interactions and the coupling between currents that include the pion cloud and currents that do not. It is assumed that these short-range contributions are already accounted for in QCD through the condensates, and their inclusion in the model would result in double counting some of the pionic effects on the nucleon correlator.

The part of the proton correlator without the pion cloud can be found in Ref. [17]. The nucleon correlator with the meson cloud for the microscopic evaluation of the sum rule has the form

$$\Pi^{(p,\pi)}(x) = D_{f,\alpha\beta}^\pi(x) \gamma^\alpha \Pi^{(p,0)}(x) \gamma^\beta, \quad (2.8)$$

where $\Pi^{(p,0)}(x)$ is the coordinate space nucleon correlator without the pion cloud [17] and in the chiral limit $D_{f,\alpha\beta}^\pi(x)$ has the form

$$D_{f,\alpha\beta}^\pi(x) = \frac{1}{\pi^2 x^4} \left(\frac{4x_\alpha x_\beta}{x^2} - \delta_{\alpha\beta} \right). \quad (2.9)$$

In momentum space the nucleon correlator with the pion cloud is

$$\Pi^{(p,\pi)}(p) = -2 \int \frac{d^4k}{(2\pi)^4} \frac{(\not{p} - \not{k}) \Pi^{(p,0)}(k) (\not{p} - \not{k})}{(p - k)^2} \quad (2.10a)$$

$$= \not{p} \Pi_{\text{odd}}^{(p,\pi)}(p) + \Pi_{\text{even}}^{(p,\pi)}(p). \quad (2.10b)$$

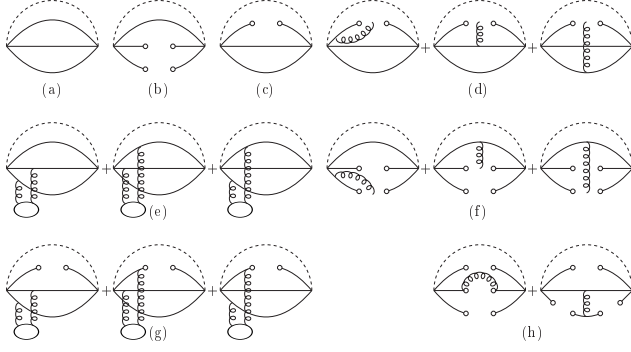


FIG. 1. The diagrams corresponding to the pion cloud contributions to the nucleon correlator in vacuum. The solid lines correspond to quarks, the helical lines to gluons and the dashed lines to Goldstone bosons. The circles and ovals correspond to the vacuum condensates.

The pion cloud contributions to the nucleon correlator are shown in the diagrams of Figure 1, and in momentum space are

$$\Pi_{1a}(p) = \frac{i}{2^{12}3 \cdot 5\pi^6\lambda_\pi^4} p^8 \ln(-p^2) \not{p} \quad (2.11a)$$

$$\Pi_{1b}(p) = \frac{i \langle \bar{q}q \rangle^2}{2^3 3 \pi^2 \lambda_\pi^4} p^2 \ln(-p^2) \not{p} \quad (2.11b)$$

$$\Pi_{1d}(p) = \frac{i \langle g_s^2 G \cdot G \rangle}{2^{11} 3 \pi^6 \lambda_\pi^4} p^4 \ln(-p^2) \not{p} \quad (2.11c)$$

$$\Pi_{1e}(p) = \frac{-i \langle \bar{q}q \rangle \langle \bar{q}g_s^2 \sigma \cdot Gq \rangle}{2^5 \pi^2 \lambda_\pi^4} \ln(-p^2) \not{p}. \quad (2.11d)$$

Details are given in Ref. [6]. The usual QCD sum rule methods are used, as in Ref. [17], but with a modification of the treatment of the continuum given by the work of Ref. [15]. In addition to the calculation of the nucleon mass the magnetic dipole moments of the nucleons were calculated. From the comparison of the results for the magnetic dipole moment to the result without the pion cloud component [19] it was estimated that the pion cloud component has roughly the same probability as the cloudless component, or $c_1^2 \simeq c_2^2 \simeq 0.5$.

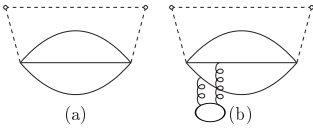


FIG. 2. The diagrams corresponding to the lowest-dimension chiral corrections to the nucleon correlator in vacuum

An important observation is that the diagrams shown in Figure 2 gives the main LNAC m_π^3 terms. The largest contribution is from the first term shown in Figure 2a, which was shown to give the following contribution to the nucleon mass

$$\begin{aligned} \Delta M_p &= -\frac{em_\pi^3 g_A^2}{160\beta^2 f_\pi^2} \\ &\simeq -20 \text{ MeV}, \end{aligned} \quad (2.12)$$

with the choice of $\lambda_\pi^2 = M_p^2/g_{\pi N}$, which is quite reasonable.

The contribution to the nucleon mass from the pion cloud was found to be negligible, consistent with the assumption $\lambda_p'^2 \ll \lambda_p^2$. We use this value for λ_π^2 in the present work. This completes the model within the uncertainty of the probability of the meson cloud component.

III. PION PROPAGATOR IN FINITE NUCLEI

Extending the model for the nucleon correlator with the pion cloud from vacuum to finite nuclei requires an appropriate modification of the pseudo-Goldstone boson field in medium. In order to be able to apply the model at high momentum transfer, which is needed for various applications, we make use of conventional multiple scattering formalism [see, e.g., Ref. [20] for a review] rather than chiral perturbation theory. This is a mean field method in which the pion propagator in the nucleon medium is given by the pion optical potential.

The propagator for a free massless pion has the form

$$D_f^\pi(k) = \frac{1}{k^2 + i\epsilon}. \quad (3.1)$$

In the medium the pion acquires an effective mass given by the optical potential. The propagator for a pion with energy k_0 in a nucleus of mass number A is

$$D_A^\pi(k) = \frac{1}{k^2 + \Pi(k_0, \vec{k}; \rho, A) + i\epsilon} \quad (3.2)$$

where $\Pi(k_0, \vec{k}; \rho, A)$ is the pion self-energy in the medium and ρ is the baryon density of the matter. The pion self energy is related to the pion-nucleus optical potential $V_{\text{opt}}(k_0)$ by

$$\Pi(k_0, \vec{k}, \vec{k}') = -2k_0 \left\langle \vec{k}' \left| V_{\text{opt}}^{\pi A}(k_0) \right| \vec{k} \right\rangle, \quad (3.3)$$

where \vec{k} and \vec{k}' are respectively the incoming and outgoing three-momenta of the pion. We begin constructing the πA optical potential by looking at the partial wave expansion of the πN scattering amplitude

$$\mathcal{F}(\vec{k}', \vec{k}) = \sum_I \hat{P}_I \left(\sum_l [(l+1) f_{I,l+}(\omega) + l f_{I,l-}(\omega)] P_l(\cos \theta) - i \vec{\sigma} \cdot (\hat{k}' \times \hat{k}) \sum_l [f_{I,l+}(\omega) - f_{I,l-}(\omega)] P_l'(\cos \theta) \right). \quad (3.4)$$

The partial wave amplitude is related to the S-matrix by

$$f_\alpha = \frac{1}{2i|\vec{k}|} (S_\alpha(\omega) - 1) \quad (3.5)$$

where the scattering matrix is found using the experimentally obtained phase shifts $\delta_\alpha(\omega)$ as

$$S_\alpha(\omega) = e^{2i\delta_\alpha(\omega)}. \quad (3.6)$$

In this notation α indexes the isospin I , orbital angular momentum l and total angular momentum J of the partial wave. The phase shifts are expected to depend on momentum proportional to k^{2l+1} , and we define the constants a_α as

$$a_\alpha = \frac{\delta_\alpha}{k^{2l+1}}. \quad (3.7)$$

These constants are the so-called scattering lengths (a_{2I}) for s-waves and the scattering volumes ($b_{2I,2J}$) for p-waves. These parameters for d-wave and higher order partial waves are very small and have negligible effect on πN physics, so we truncate the expansion of the scattering amplitude at $l = 1$. Then the πN scattering amplitude can take the form

$$\mathcal{F}(\vec{k}', \vec{k}) = a(k_0) + a_I(k_0) (\vec{t} \cdot \vec{\tau}) + [b(k_0) + b_I(k_0) (\vec{t} \cdot \vec{\tau})] \vec{k}' \cdot \vec{k} + i [b_{sf}(k_0) + b_{Isf}(k_0) (\vec{t} \cdot \vec{\tau})] \vec{\sigma} \cdot (\vec{k}' \times \vec{k}), \quad (3.8)$$

where \vec{t} and $\vec{\tau}$ are the isospin matrices for the pion and the nucleon. The energy-dependent coefficients can be related to the scattering volumes and lengths at threshold; for example, $b = \frac{1}{3} (4b_{33} + 2b_{13} + 2b_{31} + b_{11})$. Because we are concerned in this work with spin/isospin symmetric nuclei, the isospin dependent and spin-flip parts of the scattering amplitude vanish. Furthermore, the p-wave contribution is considerably larger than the s-wave contribution at low

and medium energies because of the dominance of the $\Delta(1232)$ 3,3 resonance in πN scattering. We are then left with the simple scattering amplitude for the spin and isospin averaged scattering of a pion off of a nucleon,

$$\mathcal{F}(\vec{k}', \vec{k}) = b(k_0) \vec{k}' \cdot \vec{k}. \quad (3.9)$$

In order to take into consideration the off-energy-shell effects in our optical potential, we modify the result of (3.9) by considering the p-wave t-matrix for the πN scattering in the separable form

$$\langle \vec{k}' | t_{\pi N}^{p\text{-wave}}(k_0) | \vec{k} \rangle = -b(k_0) g(\vec{k}') g(\vec{k}) \vec{k}' \cdot \vec{k}, \quad (3.10)$$

where $g(\vec{k})$ is a form-factor that roughly parametrizes the inelastic channels in the πN scattering at high energies. $g(\vec{k})$ is chosen be unity when \vec{k} is at the on-energy-shell value, and to approach zero as \vec{k} gets large, where $\bar{k} \equiv |\vec{k}|$. We use a monopole parametrization of the form factor

$$g(\vec{k}) = \frac{m_\pi^2 + \Lambda^2}{|\vec{k}|^2 + \Lambda^2}, \quad (3.11)$$

with vertex factor Λ taken to be 700 MeV, for the description of the off-shell properties of the amplitude.

The energy dependence of the function $b(k_0)$ is modelled by using the Breit-Wigner form for the $\Delta(1232)$, giving

$$b(k_0, \bar{k}) = \left(\frac{f^2 \omega_\Delta}{3\pi m_\pi^3} \right) \frac{k_0^{-1}}{\omega_\Delta - k_0 - \frac{i}{2} \Gamma_\Delta(\bar{k}, k_0)}, \quad (3.12)$$

where ω_Δ is the energy of the 3,3 resonance and f is the pseudovector πN coupling constant. We model the resonance so that the three-momentum dependence of the width Γ_Δ is cut off at low momenta and at the momentum where the resonance is saturated:

$$\Gamma_\Delta(\bar{k}, k_0) = \frac{8}{3} \frac{f^2}{4\pi} \frac{\omega_\Delta}{m_\pi^2} \frac{1}{k_0} \begin{cases} \bar{k}_m^3 & \bar{k} \leq \bar{k}_m \\ \bar{k}^3 & \bar{k}_m \leq \bar{k} \leq \bar{k}_\Delta \\ \bar{k}_\Delta^3 & \bar{k} \geq \bar{k}_\Delta \end{cases}. \quad (3.13)$$

The lower limit starting at $\bar{k}_m = 30$ MeV ensures that the $\Delta(1232)$ does not vanish even at very low pion momenta, and the upper limit at the three-momentum \bar{k}_Δ where the Breit-Wigner curve peaks provides a mechanism for the resonance to disappear at high energies as expected.

To obtain the pion-nucleus optical potential for elastic scattering we make use of three approximations:

- low density
- impulse
- local density.

The low density and impulse approximations lead to the standard first-order in ρ form for the optical potential, and the local density approximation is used for finite nuclei to treat the interaction at the nuclear surface as a function of ρ . The p-wave pion optical potential for elastic scattering by an A -nucleon nucleus can then be written to first order in density as

$$\langle \vec{k}' | V_{\text{opt}}^{\pi A} | \vec{k} \rangle = A \langle \vec{k}' | t_{\pi A}^{p\text{-wave}} | \vec{k} \rangle \tilde{\rho}(\vec{k} - \vec{k}'). \quad (3.14)$$

$\tilde{\rho}(\vec{k} - \vec{k}')$ is the Fourier transform of the ground state nuclear density $\rho(\mathbf{r})$. The resulting optical potential in coordinate space, using Eq.(3.10), has the form

$$V(\vec{r}) = A c(E_\pi) \nabla \cdot \rho(\mathbf{r}) \nabla. \quad (3.15)$$

This is the so-called Kisslinger potential [21] without the s-wave scattering term. It has been shown to give an accurate treatment of medium-energy pion-nucleus elastic scattering [20]. Due to the p-wave nature of the interaction derived

from the $\Delta(1232)$ resonance the interaction takes place mainly on the surface, and indeed vanishes in the interior of the nucleus if a constant density is used. This will be seen to be an important aspect of our present work.

We model the spatial dependence of the nuclear density as a second order harmonic oscillator

$$\rho(r) = \rho_0 \left(1 + \alpha \left(\frac{r}{c} \right)^2 \right) \exp \left(- \left(\frac{r}{c} \right)^2 \right), \quad (3.16)$$

where ρ_0 is the density of nuclear matter, c is a size parameter, and α provides some control over the shape, allowing for modelling of heavier nuclei (like ^{40}Ca) and more complicated distributions (for example, ^{16}O with a local minimum at the center).

We now turn our attention to the pion propagator in medium. The propagator (3.2) is expanded in density as

$$D_A^\pi(k) = [D_A^\pi(k)]_{\rho_0=0} + \sum_{\vec{q}} \tilde{\rho}(\vec{q}) \left[\frac{\delta}{\delta \tilde{\rho}(\vec{q})} D_A^\pi(k) \right]_{\rho_0=0} + \frac{1}{2!} \sum_{\vec{q}_1} \sum_{\vec{q}_2} \tilde{\rho}(\vec{q}_1) \tilde{\rho}(\vec{q}_2) \left[\frac{\delta}{\delta \tilde{\rho}(\vec{q}_1)} \frac{\delta}{\delta \tilde{\rho}(\vec{q}_2)} D_A^\pi(k) \right]_{\rho_0=0} + \dots \quad (3.17)$$

where the first term is just the free pion propagator (3.1) and \vec{q} is the momentum transfer in the scattering. The scattering angles are averaged over, and the pion propagator in the nucleus takes the form

$$D_A^\pi(k) = D_f^\pi(k) + \frac{8\pi^{3/2}(A-1)\rho_0 f^2 \omega_\Delta}{m_\pi^2 c} g(\bar{k})^2 F_1(\bar{k}, \alpha, c) \left(\omega_\Delta - k_0 - \frac{i}{2} \Gamma_\Delta(\bar{k}, k_0) \right)^{-1} D_f^\pi(k)^2 + \mathcal{O}(\rho_0^2), \quad (3.18)$$

with the nuclear structure information contained in the function

$$F_1(\bar{k}, \alpha, c) = \left(1 + \frac{3\alpha}{2} \right) \left[\left(1 - \frac{2}{c^2 \bar{k}^2} \right) + \left(2c^2 \bar{k}^2 + 3 + \frac{2}{c^2 \bar{k}^2} \right) \exp(-c^2 \bar{k}^2) \right] - \alpha \left[\left(1 - \frac{3}{c^2 \bar{k}^2} \right) + \left(2c^4 \bar{k}^4 + 4c^2 \bar{k}^2 + 5 + \frac{3}{c^2 \bar{k}^2} \right) \exp(-c^2 \bar{k}^2) \right]. \quad (3.19)$$

IV. THE NUCLEON CORRELATOR WITH PION CLOUD IN MEDIUM

To construct the in-medium nucleon correlator with the meson field, we start by rewriting the vacuum matrix element of the product $\eta(x)\bar{\eta}(x)$ in Eq.(2.7) as a nuclear matrix element so that the proton current correlator takes the form

$$\begin{aligned} \Pi_A^p(p) &= i \int d^4x e^{ip \cdot x} \langle A | T [\eta^p(x) \bar{\eta}^p(0)] | A \rangle \\ &= c_1^2 i \int d^4x e^{ip \cdot x} \langle A | T [\eta^{p,0}(x) \bar{\eta}^{p,0}(0)] | A \rangle + c_2^2 i \int d^4x e^{ip \cdot x} \langle A | T [\eta^{p,\pi}(x) \bar{\eta}^{p,\pi}(0)] | A \rangle \\ &= c_1^2 \Pi_A^{(p,0)}(p) + c_2^2 \Pi_A^{(p,\pi)}(p), \end{aligned} \quad (4.1)$$

where $|A\rangle$ is the ground state of the finite nucleus. The part of the in-medium proton correlator with the pseudo-Goldstone field is

$$\begin{aligned} \Pi_A^{(p,\pi)}(x) &= \epsilon^{abc} \epsilon^{a'b'c'} \frac{1}{\lambda_\pi^4} \left\{ \frac{2}{3} \left(\partial_\alpha \partial_\beta D_A^{\pi^0}(x) \right) \gamma_\alpha \gamma^\mu S_{d,A}^{cc'}(x) \gamma^\nu \gamma_\beta \text{Tr} \left[S_{u,A}^{bb'}(x) \gamma_\nu C S_{u,A}^{aa'T}(x) C \gamma_\mu \right] \right. \\ &\quad \left. + \frac{4}{3} \left(\partial_\alpha \partial_\beta D_A^{\pi^+}(x) \right) \gamma_\alpha \gamma^\mu S_{u,A}^{cc'}(x) \gamma^\nu \gamma_\beta \text{Tr} \left[S_{d,A}^{bb'}(x) \gamma_\nu C S_{d,A}^{aa'T}(x) C \gamma_\mu \right] \right\} \\ &\quad + [\text{4-quark terms}] \\ &= \frac{1}{\lambda_\pi^4} \left\{ \frac{2}{3} D_{A,\alpha\beta}^{\pi^0}(x) \gamma^\alpha \Pi_A^{(p,0)}(x) \gamma^\beta + \frac{4}{3} D_{A,\alpha\beta}^{\pi^+}(x) \gamma^\alpha \Pi_A^{(n,0)}(x) \gamma^\beta \right\}. \end{aligned} \quad (4.2)$$

This is simply the expression for the meson cloud part of the correlator, given in Ref. [6], where the quark propagator and pion propagator in vacuum, $S_q^{ab}(x)$ and $D_f^\pi(x)$, are replaced by $S_{q,A}^{ab}(x)$ and $D_A^\pi(x)$, the quark and pion propagators in the nucleus, respectively. For example,

$$S_{q,A}^{ab}(x) = \langle A | T [q^a(x) \bar{q}^b(0)] | A \rangle. \quad (4.3)$$

$D_{A,\alpha\beta}^\pi(x)$ is the nuclear analogue to Eq.(2.9), replacing the free pion propagator $D_f^\pi(x)$ with $D_A^\pi(x)$. As with the case in vacuum, the neutron correlator $\Pi_A^{(n,0)}(x)$ is found simply by an interchange of up and down quark fields in the current $\eta(x)$. With a spin/isospin symmetric nucleus in the chiral limit, the in-medium correlator with a pion cloud has the form analogous to Eq.(2.8),

$$\Pi_A^{(p,\pi)}(x) = \frac{2}{\lambda_\pi^4} D_{A,\alpha\beta}^\pi(x) \gamma^\alpha \Pi_A^{(p,0)}(x) \gamma^\beta. \quad (4.4)$$

For simplicity we work in momentum space, where the in-medium proton correlator has the form

$$\Pi_A^p(p) = c_1^2 \Pi_A^{(p,0)}(p) - (1 - c_1^2) \frac{2}{\lambda_\pi^4} \int \frac{d^4 k}{(2\pi)^4} D_A^\pi(k) \not{k} \Pi_A^{(p,0)}(p - k) \not{k} \quad (4.5)$$

where we made use of the Fourier transform of $D_{A,\alpha\beta}^\pi(x)$:

$$D_{A,\alpha\beta}^\pi(p) = -p_\alpha p_\beta D_A^\pi(p). \quad (4.6)$$

Since the nucleus has a four-momentum u^μ , breaking Lorentz invariance, there are additional Dirac structures in the nucleon correlator. Under the assumption that the nuclear ground state is invariant under parity and time-reversal, it was shown [1] that the in-medium nucleon correlator is

$$\Pi_A^p(p) = \Pi_A^{(s)}(p^2, p \cdot u) + \Pi_A^{(p)}(p^2, p \cdot u) \not{p} + \Pi_A^{(u)}(p^2, p \cdot u) \not{u}. \quad (4.7)$$

The individual scalar functions $\Pi_A^{(n)}(p^2, p \cdot u)$ depend only on the Lorentz invariants p^2 and $p \cdot u$ and can be projected out of the full nucleon correlator using the following formulae [1,22]:

$$\begin{aligned} \Pi_A^{(s)}(p^2, p \cdot u) &= \frac{1}{4} \text{Tr} [\Pi_A^p(p)] \\ \Pi_A^{(p)}(p^2, p \cdot u) &= \frac{1}{p^2 - (p \cdot u)^2} \left[\frac{1}{4} \text{Tr} [\not{p} \Pi_A^p(p)] - \frac{p \cdot u}{4} \text{Tr} [\not{u} \Pi_A^p(p)] \right] \\ \Pi_A^{(u)}(p^2, p \cdot u) &= \frac{1}{p^2 - (p \cdot u)^2} \left[\frac{1}{4} \text{Tr} [\not{u} \Pi_A^p(p)] - \frac{p \cdot u}{4} \text{Tr} [\not{p} \Pi_A^p(p)] \right]. \end{aligned} \quad (4.8)$$

We define in-medium matrix elements of an operator $\mathcal{O}(x)$ as an expansion in local nuclear density ρ

$$\begin{aligned} \langle \mathcal{O}(x) \rangle_\rho &= \langle A | \mathcal{O}(x) | A \rangle - \langle 0 | \mathcal{O}(x) | 0 \rangle \\ &= \rho \langle N | \mathcal{O}(x) | N \rangle + \dots, \end{aligned} \quad (4.9)$$

where $\langle N | \mathcal{O}(x) | N \rangle$ is the single-nucleon matrix element of $\mathcal{O}(x)$. The in-medium quark condensate is related to the π - N sigma commutator by [1]

$$\langle \bar{q}q \rangle_\rho = \rho \frac{\sigma_{\pi N}}{m_u + m_d}. \quad (4.10)$$

We take $\sigma_{\pi N} \simeq 47$ MeV [23]. The breaking of the Lorentz invariance of the medium by the introduction of the nuclear four-momentum u^μ leads to condensates with additional Dirac structures. The dimension three in-medium vector quark condensate, with the appropriate color and flavor weighting, is proportional to the nuclear density

$$\langle q^\dagger q \rangle_\rho = \frac{3}{2} \rho. \quad (4.11)$$

The in-medium gluon condensate is found via the trace anomaly [24,25] to be

$$\langle g_s^2 G_{\mu\nu} G^{\mu\nu} \rangle_\rho = -\rho 2^6 39 \pi^2 \text{ MeV}. \quad (4.12)$$

The values of the five-dimensional mixed quark-gluon condensates in medium are not well known, although significant cancellation between diagrams containing these matrix elements occurs much like similar terms in the free nucleon correlator in the chiral limit. Furthermore, it was shown in [22] that the nucleon sum rules are insensitive to the values of these condensates, so we ignore terms proportional to the mixed condensates in our sum rule analysis.

The nucleon correlator is analyzed in the rest frame of the nucleus, where the nucleus four-momentum is $u = (M, 0, 0, 0)$ with the mass of the nucleus $M \approx Am$ (neglecting the average binding energy per nucleon in the nucleus as small compared to the nucleon mass m). In this frame $p \cdot u = 2Mp_0$, where p_0 is the energy of the interpolating field. We carry out Borel transforms with respect to $-p^2$, using the relationship

$$\left(\frac{M}{A} + p\right)^2 = 4m^2. \quad (4.13)$$

In the nuclear rest frame, $p_0 = \frac{1}{2m}(3m^2 - p^2)$, so when $-p^2 \rightarrow \infty$, $p \cdot u \rightarrow \infty$ while the ratio of the two invariants, analogous to the Bjorken scaling variable in DIS, remains fixed and the OPE is applicable.

We restrict our calculation of the nucleon correlator to first order in the nuclear density. We can then identify three distinct types of quark current diagrams that contribute to the correlator: diagrams that contribute to the part of the in-medium correlator without the pseudo-Goldstone field (Figure 3), diagrams that include the pion field where the quarks and gluons interact with the medium and the pion maintains its in-vacuum properties (Figure 4), and diagrams where the quarks and glue interact with the QCD vacuum and the pion scatters in the nucleus (Figure 5). The shaded boxes in these diagrams represent interaction of the field with the nuclear medium to first order in the density expansion. Diagrams where the quarks and pions both interact with the medium, or where the pion scattering includes two-body correlations would come in at second order in density and are not included in this work.

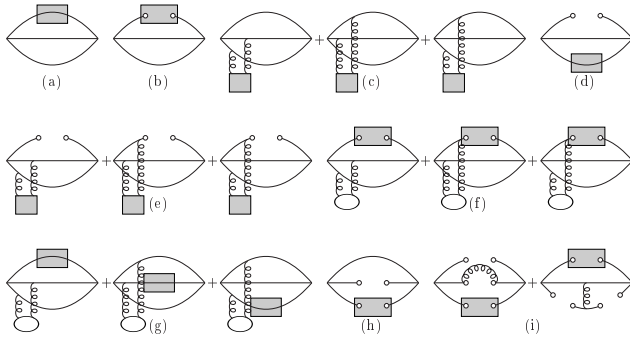


FIG. 3. The diagrams corresponding to the contributions to the nucleon correlator in medium without the pion cloud. The shaded boxes represent the interaction of the fields with the medium to first order in density.

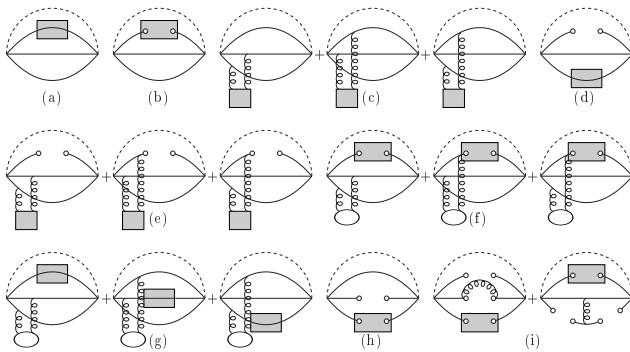


FIG. 4. The diagrams corresponding to the free pion cloud contributions to the nucleon correlator in medium.

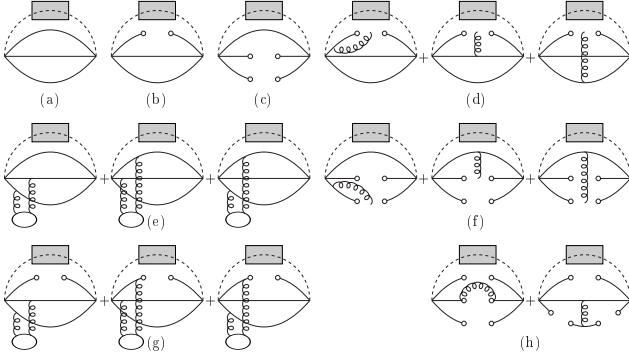


FIG. 5. The diagrams corresponding to the in-medium pion cloud contributions to the nucleon correlator in medium.

The first two sets of diagrams are most easily calculated in coordinate space using (4.4), after which they are Fourier transformed into momentum space. The contributions at first order in the density from diagrams without the pion cloud are found to be [1,22]

$$\begin{aligned}
\Pi_{(2a,\rho)}(p) &= \frac{i}{3\pi^2} \langle q^\dagger q \rangle_\rho [2\not{p}p^2 + \not{p}u \cdot p] \ln(-p^2) \\
\Pi_{(2b,\rho)}(p) &= \frac{i}{(2\pi)^2} \langle \bar{q}q \rangle_\rho p^2 \ln(-p^2) \\
\Pi_{(2c,\rho)}(p) &= -\frac{i}{2^7\pi^4} \langle g_s^2 G \cdot G \rangle_\rho \not{p} \ln(-p^2) \\
\Pi_{(2d,\rho)}(p) &= -\frac{2^2 i}{3} \langle \bar{q}q \rangle_\rho \langle q^\dagger q \rangle_\rho \frac{u \cdot p}{p^2} \\
\Pi_{(2e+2f,\rho)}(p) &= -\frac{i}{3^2 2\pi^2} \left[\langle \bar{q}q \rangle_\rho \langle g_s^2 G \cdot G \rangle_\rho + \langle \bar{q}q \rangle_\rho \langle g_s^2 G \cdot G \rangle_\rho \right] \frac{1}{p^2} \\
\Pi_{(2g,\rho)}(p) &= \frac{i}{2^5 3^2 \pi^2} \langle q^\dagger q \rangle_\rho \langle g_s^2 G \cdot G \rangle_\rho \left[5\not{p} \frac{1}{p^2} - 2\not{p} \frac{u \cdot p}{p^4} \right] \\
\Pi_{(2h,\rho)}(p) &= -\frac{2^2 i}{3} \langle \bar{q}q \rangle_\rho \langle \bar{q}q \rangle_\rho \not{p} \frac{1}{p^2} \\
\Pi_{(2i,\rho)}(p) &= -\frac{2^2 17 i}{3^3} g_s^2 \langle \bar{q}q \rangle_\rho^2 \langle \bar{q}q \rangle_\rho \frac{1}{p^4}.
\end{aligned} \tag{4.14}$$

Here we have used a factorization approximation to evaluate the effects of the four-quark and six-quark condensates, where to first order in density we take $\langle \bar{q}\Gamma q \bar{q}\Gamma q \rangle_\rho \approx \langle \bar{q}q \rangle_\rho \langle \bar{q}q \rangle_\rho$ and $\langle \bar{q}\Gamma q \bar{q}\Gamma q \bar{q}\Gamma q \rangle_\rho \approx \langle \bar{q}q \rangle_\rho^2 \langle \bar{q}q \rangle_\rho$, respectively. While the factorization of these condensates is unjustified in medium [26], our primary concern is a comparison of the nucleon mass shift due to the pion cloud terms and the shift due to terms without the pion cloud, so we find the approximation acceptable for the problem at hand.

The diagrams in Figure 4, where there are first-order interactions of the quarks and gluons with the medium but the pions interact only with the vacuum, provide the following contributions at first order in the density:

$$\begin{aligned}
\Pi_{(3a,\rho)}(p) &= -\frac{i}{2^6 3^2 \pi^4 \lambda_\pi^4} \langle q^\dagger q \rangle_\rho [\not{p}p^2 + 3\not{p}u \cdot p] p^4 \ln(-p^2) \\
\Pi_{(3c,\rho)}(p) &= \frac{i}{2^{13} \pi^6 \lambda_\pi^4} \langle g_s^2 G \cdot G \rangle_\rho \not{p} p^4 \ln(-p^2) \\
\Pi_{(3g,\rho)}(p) &= -\frac{i}{2^8 3^3 \pi^4 \lambda_\pi^4} \langle q^\dagger q \rangle_\rho \langle g_s^2 G \cdot G \rangle_\rho [2 \cdot 5\not{p}p^2 + 11\not{p}u \cdot p] \ln(-p^2) \\
\Pi_{(3h,\rho)}(p) &= \frac{i}{2^2 3 \pi^2 \lambda_\pi^4} \langle \bar{q}q \rangle_\rho \langle \bar{q}q \rangle_\rho \not{p} p^2 \ln(-p^2).
\end{aligned} \tag{4.15}$$

All diagrams which would be expected to contribute to scalar structure of the nucleon correlator vanish.

The calculation of the terms represented in Figure 5 where the pions interact with the nucleus and the quarks and glue interact within the QCD vacuum are more difficult to calculate. Instead of calculating these diagrams in coordinate space as we did with the other in-medium diagrams, which would require first a rather daunting Fourier transform of the in-medium pion propagator (Eq. 3.18) and then an inverse transform of the resulting expression, we perform the calculations in momentum space using Equation (4.5) as the starting point. For example, the term corresponding to Figure 5a gives the linear-density contribution

$$\Pi_{(4a,\rho)}(p) = \frac{\zeta^i}{2^{10}\pi^8\lambda_\pi^4} \int d^3\vec{k} (g(\vec{k}))^2 F_1(\vec{k}, \alpha, c) \\ \times \int dk_0 k_0 \frac{(\omega_\Delta - k_0) k_0 + \frac{i}{2}\Gamma_\Delta(\vec{k})}{(\omega_\Delta - k_0)^2 k_0^2 + \frac{1}{4}(\Gamma_\Delta(\vec{k}))^2} \frac{(p-k)^4 \ln[-(p-k)^2]}{(k_0^2 - \vec{k}^2 + i\epsilon)^2} [(2p \cdot k - k^2) \not{k} - k^2 \not{p}]$$

where $\zeta = \frac{8\pi^{\frac{3}{2}}(A-1)\rho_0 f_\pi^2 \omega_\Delta}{m_\pi^2 c}$. The Borel transform with respect to $-p^2$, \hat{B} , eliminates terms proportional to $p \cdot k$ in the expansion of $(p-k)^{2n} \ln[-(p-k)^2]$, simplifying the integrand so that the term proportional to \not{k} vanishes from symmetry in the angle-averaging. We are left with integrals over the pion energy k_0 and the magnitude of the pion three-momentum \vec{k} . The integrand also picks up a Borel dependence of the form $M_B^{2n} \exp(-k^2/M_B^2)$. The energy integration can be completed analytically, where we find that the factor $\exp(-k^2/M_B^2) \rightarrow 1$ and the dependence on the Borel mass can be taken out of the integral. This first diagram is found to be

$$\hat{B}\Pi_{(4a,\rho)}(p) = \frac{\zeta^i}{\lambda_\pi^4} I(\alpha, c) \frac{1}{(2\pi)^7} \not{p} M_B^6 \quad (4.16)$$

where $I(\alpha, c)$ is the remaining one-dimensional integral over the pion three-momentum. Defining $\tilde{\Gamma}(\vec{k}) = k_0 \Gamma(\vec{k}, k_0)$, the integral takes the form

$$I(\alpha, c) = \frac{-i}{2\pi^2 c^2} \int_0^\infty d\vec{k} F_1(\vec{k}, \alpha, c) (g(\vec{k}))^2 \frac{\omega_\Delta \vec{k} - \vec{k}^2 + \frac{i}{2}\tilde{\Gamma}(\vec{k})}{(\omega_\Delta \vec{k} - \vec{k}^2)^2 + \frac{1}{4}(\tilde{\Gamma}(\vec{k}))^2}. \quad (4.17)$$

We calculate this integral numerically.

The other diagrams shown in Figure 5 yield the following contributions to the nucleon correlator:

$$\begin{aligned} \hat{B}\Pi_{(4b,\rho)}(p) &= -\frac{\zeta^i}{\lambda_\pi^4} I(\alpha, c) \frac{4\pi}{(2\pi)^6} \langle \bar{q}q \rangle M_B^4 \\ \hat{B}\Pi_{(4c,\rho)}(p) &= \frac{\zeta^i}{\lambda_\pi^4} I(\alpha, c) \frac{2^3\pi}{(2\pi)^4 3} \not{p} \langle \bar{q}q \rangle^2 \\ \hat{B}\Pi_{(4e,\rho)}(p) &= -\frac{\zeta^i}{\lambda_\pi^4} I(\alpha, c) \frac{1}{2^9\pi^7} \not{p} \langle g_s^2 G \cdot G \rangle M_B^2 \\ \hat{B}\Pi_{(4f,\rho)}(p) &= -\frac{\zeta^i}{\lambda_\pi^4} I(\alpha, c) \frac{1}{2^4 3\pi^7} \not{p} \langle \bar{q}q \rangle \langle \bar{q}g_s \sigma \cdot Gq \rangle \frac{1}{M_B^2} \\ \hat{B}\Pi_{(4g,\rho)}(p) &= -\frac{\zeta^i}{\lambda_\pi^4} I(\alpha, c) \frac{1}{2^3 3^2 \pi^5} \langle \bar{q}q \rangle \langle g_s^2 G \cdot G \rangle \\ \hat{B}\Pi_{(4h,\rho)}(p) &= \frac{\zeta^i}{\lambda_\pi^4} I(\alpha, c) \frac{17}{3^4 \pi^3} g_s^2 \langle \bar{q}q \rangle^3 \frac{1}{M_B^2}, \end{aligned} \quad (4.18)$$

where $I(\alpha, c)$ in each of these expressions is the same as Equation (4.17).

V. CONSTRUCTION OF THE IN-MEDIUM SUM RULES

A. In the Chiral Limit

The phenomenological (“right-hand”) side of the sum rules, is expressed as a dispersion relation with a lowest-lying hadronic pole of in-medium mass m^* and residue λ_p^{*2} clearly separated from a continuum of higher-energy states with threshold s_0^* [1]:

$$\Pi_{A,\text{RHS}}^p(p) = \lambda_p^{*2} c_1^2 \frac{\not{p} + m^*}{p^2 - m^{*2}} + \frac{1}{\pi} \int_{s_0^*}^{\infty} ds \frac{\text{Im}\Pi_A^{\text{cont}}(s, u \cdot q)}{s - p^2} \quad (5.1)$$

Guided by the vacuum calculations, we assume that the structure parameter associated with the current including the pion cloud $\lambda_p'^{*2} \ll \lambda_p^{*2}$, so there is no additional pole considered in our model of the phenomenological correlator. Rather than find the values of the parameters in medium, we follow the approach of Drukarev and Levin and determine the shifts of the in-medium parameters from their vacuum values [1]. We remove the contributions to the nucleon correlator due to the pure in-vacua diagrams by defining the quantity

$$\phi^{(i)} \equiv -2i (2\pi)^4 \hat{B} \left[\Pi_A^{(i)}(p) - \Pi^{(i)}(p) \right], \quad (5.2)$$

where i labels the three structures in the sum rule (**1**, \not{p} , and \not{u} , respectively). On the phenomenological side of the sum rule we can express $\phi^{(i)}$ in terms of the parameter shifts and the Borel transform of the RHS in vacuum as

$$\phi^{(i)}(M_B^2, s) = \left[\Delta m \frac{\partial}{\partial m} + \Delta \tilde{\lambda}^2 \frac{\partial}{\partial \tilde{\lambda}^2} + \Delta s_0 \frac{\partial}{\partial s_0} \right] \hat{B} \Pi_{0,\text{RHS}}^{(i)}(p) \quad (5.3)$$

for $i = s, p$ (since there is no u structure in vacuum). The contributions to the microscopic side of the sum rule are given in the previous section. With the subscript labelling the contributions due to each figure, we find in the nuclear rest frame using the constraint in Equation (4.13):

$$\begin{aligned} \phi_2^{(s)}(M_B^2) &= 2\rho a_N M_B^4 E_1 + \left[-3 \cdot 2^3 \pi^2 \rho m^2 a_0 - \frac{2^2}{3^2} \rho (b_N a_0 + b_0 a_N) \right] + \frac{2 \cdot 17}{3^2 \pi^2} g_s^2 \rho a_0^3 \frac{1}{M_B^2} \\ \phi_2^{(p)}(M_B^2) &= 2^4 \pi^2 \rho M_B^4 E_1 L^{-\frac{4}{9}} + \left[\frac{1}{2^2} \rho b_N - \frac{2^4 \pi^2}{3} m^2 \rho \right] M_B^2 E_0 L^{-\frac{4}{9}} + \left[\frac{2^3}{3} \rho a_0 a_N L^{\frac{4}{9}} - \frac{\pi^2}{3 \cdot 2} \rho b_0 L^{-\frac{4}{9}} \right] \\ &\quad - \pi^2 \rho b_0 m^2 L^{-\frac{4}{9}} \frac{1}{M_B^2} \\ \phi_2^{(u)}(M_B^2) &= -2^6 \pi^2 \rho M_B^4 E_1 L^{-\frac{4}{9}} - \frac{5\pi^2}{3 \cdot 2} \rho b_0 L^{-\frac{4}{9}} \end{aligned} \quad (5.4a)$$

$$\begin{aligned} \phi_3^{(s)}(M_B^2) &= 0 \\ \phi_3^{(p)}(M_B^2) &= \frac{1}{\lambda_\pi^4} \left(-\frac{3}{2^2} \rho M_B^8 E_3 L^{-\frac{4}{9}} + \left[\frac{3}{2^2} m^2 \rho - \frac{1}{2^7 \pi^2} \rho b_N \right] M_B^6 E_2 L^{-\frac{4}{9}} \right. \\ &\quad \left. + \left[-\frac{1}{2 \cdot 3 \pi^2} \rho a_0 a_N L^{\frac{4}{9}} - \frac{11\pi^4}{2^5 3^2} \rho b_0 L^{-\frac{4}{9}} \right] M_B^4 E_1 + \frac{11\pi^4}{2^5 3^2} \rho b_0 M_B^2 E_0 L^{-\frac{4}{9}} \right) \\ \phi_3^{(u)}(M_B^2) &= \frac{1}{\lambda_\pi^4} \left(\frac{3}{2} \rho M_B^8 E_3 L^{-\frac{4}{9}} + \frac{5}{2^3 3^2} \rho b_0 M_B^4 E_1 L^{-\frac{4}{9}} \right) \end{aligned} \quad (5.4b)$$

$$\begin{aligned} \phi_4^{(s)}(M_B^2) &= \frac{\zeta}{\lambda_\pi^4} \text{Re}[I(\alpha, c)] \left[\frac{a_0}{\pi^3} M_B^4 E_1 + \frac{2a_0 b_0}{3^2 \pi^3} - \frac{17}{3^4 \pi^5} g_s^2 a_0^3 \frac{1}{M_B^2} \right] \\ \phi_4^{(p)}(M_B^2) &= \frac{\zeta}{\lambda_\pi^4} \text{Re}[I(\alpha, c)] \left[\frac{1}{2\pi^3} M_B^6 E_2 L^{-\frac{4}{9}} - \frac{b_0}{2^3 \pi^3} M_B^2 E_0 L^{-\frac{4}{9}} + \frac{2a_0^2}{3\pi^3} L^{\frac{4}{9}} - \frac{a_0^2 m_0^2}{3 \cdot 2^2 \pi^7} \frac{1}{M_B^2} \right] \\ \phi_4^{(u)}(M_B^2) &= 0. \end{aligned} \quad (5.4c)$$

Here we have used for the condensates

$$\begin{aligned} a_0 &= -(2\pi)^2 \langle \bar{q}q \rangle = 0.55 \text{ GeV}^3, \\ a_N &= -(2\pi)^2 \langle N | \bar{q}q | N \rangle, \\ b_0 &= \langle g_s^2 G \cdot G \rangle = 0.474 \text{ GeV}^4, \\ b_N &= \langle N | g_s^2 G \cdot G | N \rangle, \text{ and} \\ m_0^2 &= \frac{\langle \bar{q}g_s \sigma \cdot G q \rangle}{a_0} = 0.8 \text{ GeV}^2. \end{aligned}$$

The left-hand side of the sum rule is then $\phi^{(i)} = c_1^2 \phi_2^{(i)} - c_2^2 \phi_3^{(i)} - c_2^2 \phi_4^{(i)}$. We have taken into account perturbative corrections using the renormalization group anomalous dimensions of the interpolating field and the local operators

used in constructing the LHS. Each term is multiplied by the appropriate power of the anomalous dimension factor [17,19]

$$L \equiv \frac{\ln(M_B/\Lambda_{\text{QCD}})}{\ln(\mu/\Lambda_{\text{QCD}})}. \quad (5.5)$$

Since it arises from a conserved current, the anomalous dimension of the pseudo-Goldstone boson is zero. We set the renormalization point of the OPE $\mu = 500$ MeV and the QCD scale parameter $\Lambda_{\text{QCD}} = 100$ MeV. In the continuum model, the contributions from higher-energy states are included by using the prescription whereby terms proportional to M_B^{2n} are multiplied by factors of E_{n-1} defined as

$$E_n \equiv 1 - \exp(-s_0^*/M_B^2) \sum_{k=0}^n \frac{1}{k!} \left(\frac{s_0^*}{M_B^2} \right)^k. \quad (5.6)$$

We introduce a pair of functions $\Phi^{(i)}$ as

$$\begin{aligned} \Phi^{(s)}(M_B^2, s) &= \phi^{(s)}(M_B^2, s) \\ &= c_1^2 \left\{ \tilde{\lambda}^2 \left(1 - \frac{2m^2}{M_B^2} \right) e^{-\frac{m^2}{M_B^2}} \Delta m + m e^{-\frac{m^2}{M_B^2}} \Delta \tilde{\lambda}^2 - 2as_0 e^{-\frac{s_0}{M_B^2}} \Delta s_0 \right\} \end{aligned} \quad (5.7)$$

$$\begin{aligned} \Phi^{(p)}(M_B^2, s) &= -m\phi^{(p)}(M_B^2, s), \\ &= c_1^2 \left\{ \frac{2m^2}{M_B^2} \tilde{\lambda}^2 e^{-\frac{m^2}{M_B^2}} \Delta m - m e^{-\frac{m^2}{M_B^2}} \Delta \tilde{\lambda}^2 \right. \\ &\quad \left. + \frac{m}{2} L^{-\frac{4}{9}} \left[\frac{s_0^4}{\lambda_\pi^4 3 \cdot 2^5 5} + s_0^2 \left(1 - \frac{b}{\lambda_\pi^4 3 \cdot 2^5} \right) + \frac{a^2 L^{\frac{8}{9}} s_0}{\lambda_\pi^4 3 \cdot 2^2} + \left(\frac{b}{2} + \frac{m_0^2 a^2}{\lambda_\pi^4 3 \cdot 2^2} \right) \right] e^{-\frac{s_0}{M_B^2}} \Delta s_0 \right\}. \end{aligned} \quad (5.8)$$

The sum of these functions has no dependence on the residue shift $\Delta \tilde{\lambda}^2$, and sufficient cancellation occurs between the terms proportional to the threshold shift Δs_0 that we can ignore these terms. The in-nucleus mass shift of the nucleon can then be determined using

$$\Delta m = \frac{1}{c_1^2 \tilde{\lambda}^2} \exp\left(\frac{m^2}{M_B^2}\right) \left[\Phi^{(s)}(M_B^2, s) + \Phi^{(p)}(M_B^2, s) \right]. \quad (5.9)$$

We adopt a derivative improvement to the sum rules suggested by Drukarev and Ryskin [27] where

$$\psi_j^{(i)} \equiv \frac{M_B^4}{m^2} \frac{d\phi_j^{(i)}}{dM_B^2}. \quad (5.10)$$

This improvement minimizes the effect of the factorization approximation of the four quark condensates by eliminating the terms proportional to p^{-2} from the dominant contributing diagrams, therefore aiding the convergence of the sum rules. Applying the derivative operator to Equations (5.4) we find

$$\begin{aligned} \psi_2^{(s)}(M_B^2) &= 2^2 \rho a_N \frac{1}{m^2} M_B^6 E_2 - \frac{1}{m^2} \frac{2 \cdot 17}{3^3 \pi^2} g_s^2 \rho a_0^3 \\ \psi_2^{(p)}(M_B^2) &= 2^5 \pi^2 \rho \frac{1}{m^2} M_B^6 E_2 L^{-\frac{4}{9}} + \left[\frac{1}{2^2} \rho b_N \frac{1}{m^2} - \frac{2^4 \pi^2}{3} \rho \right] M_B^4 E_1 L^{-\frac{4}{9}} + \pi^2 \rho b_0 L^{-\frac{4}{9}} \\ \psi_2^{(u)}(M_B^2) &= -2^7 \pi^2 \rho \frac{1}{m^2} M_B^6 E_2 L^{-\frac{4}{9}} \\ \psi_3^{(s)}(M_B^2) &= 0 \\ \psi_3^{(p)}(M_B^2) &= \frac{1}{\lambda_\pi^4} \left(-\frac{3}{m^2} \rho M_B^{10} E_4 L^{-\frac{4}{9}} + \left[\frac{3^2}{2^2} \rho - \frac{3}{2^7 \pi^2} \frac{\rho b_N}{m^2} \right] M_B^8 E_3 L^{-\frac{4}{9}} \right. \\ &\quad \left. + \left[-\frac{1}{3\pi^2} \rho \frac{a_0 a_N}{m^2} L^{\frac{4}{9}} - \frac{11\pi^4}{2^4 3^2} \frac{\rho b_0}{m^2} L^{-\frac{4}{9}} \right] M_B^6 E_2 + \frac{11\pi^4}{2^5 3^2} \frac{\rho b_0}{m^2} M_B^4 E_1 L^{-\frac{4}{9}} \right) \end{aligned} \quad (5.11a)$$

$$\begin{aligned}
\psi_3^{(u)}(M_B^2) &= \frac{1}{\lambda_\pi^4} \left(\frac{3 \cdot 2}{m^2} \rho M_B^{10} E_4 L^{-\frac{4}{9}} + \frac{5}{2^3 3^2} \rho \frac{b_0}{m^2} M_B^6 E_2 L^{-\frac{4}{9}} \right) \\
\psi_4^{(s)}(M_B^2) &= \frac{\zeta}{\lambda_\pi^4} \text{Re}[I(\alpha, c)] \left[\frac{2a_0}{m^2 \pi^3} M_B^6 E_2 + \frac{17}{3^4 \pi^5} \frac{g_s^2}{m^2} a_0^3 \right] \\
\psi_4^{(p)}(M_B^2) &= \frac{\zeta}{\lambda_\pi^4} \text{Re}[I(\alpha, c)] \left[\frac{3}{2\pi^3} \frac{1}{m^2} M_B^8 E_3 L^{-\frac{4}{9}} - \frac{b_0}{2^3 \pi^3} \frac{1}{m^2} M_B^4 E_1 L^{-\frac{4}{9}} + \frac{a_0^2 m_0^2}{3 \cdot 2^2 \pi^7} \frac{1}{m^2} \right] \\
\psi_4^{(u)}(M_B^2) &= 0
\end{aligned} \tag{5.11b}$$

$$\tag{5.11c}$$

The improvement does not remove all dependence of the LHS on the four-quark condensate, but these remaining four-quark terms are largely suppressed in comparison to terms with similar Borel weighings. As with the unimproved sum rules, a linear combination of these expressions can be built that has no dependence on the residue shift and negligible dependence on the threshold shift, giving the mass shift of the nucleon as

$$\Delta m = \frac{1}{c_1^2 \lambda^2} \exp\left(\frac{m^2}{M_B^2}\right) \left[\psi^{(s)}(M_B^2, s) - m \psi^{(p)}(M_B^2, s) \right]. \tag{5.12}$$

The improved sum rule is used in the analysis of the nucleon mass shifts in this work.

B. Beyond the Chiral Limit

As discussed above, in Ref. [6] it was shown that processes illustrated in Figure 2 produce terms proportional to m_π^3/f_π^2 . Also the $m_\pi^2 \ln(m_\pi^2)$ terms were shown to cancel using the analysis of Ref. [15]. It was thereby shown that our pion cloud model is consistent with chiral perturbation theory to leading order in the nonanalytic contributions to the nucleon mass in vacuum, and that we could use the chiral perturbation theory result to constrain the parameters of the model

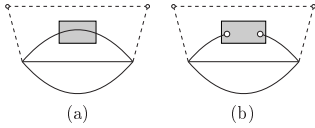


FIG. 6. The diagrams corresponding to the lowest-dimension chiral corrections to the nucleon correlator in medium.

In dense nuclear matter (and at finite temperature, Refs. [28,29]) another problem with chiral symmetry breaking seems to occur in the QCD sum rule method [16]. Equation (4.10) can be rewritten as

$$\frac{\langle \bar{q}q \rangle_\rho}{\langle \bar{q}q \rangle_0} = -\rho \frac{\sigma_{\pi N}}{f_\pi^2 m_\pi^2}. \tag{5.13}$$

However, the LNAC to the πN sigma commutator is proportional to m_π^3 [23]). The leading nonanalytic contribution to the in-medium quark condensate is thereby seen to be of order ρm_π , which is forbidden by chiral counting rules [30]. Birse and Krippa accounted for this by adding contributions to the RHS where the nucleon current interacts with soft pions from the pion cloud of another nucleon in the nucleus [16]. Using the soft pion theorem of PCAC [31] they find a term proportional to ρm_π on the phenomenological side which cancels the offending term on the microscopic side arising from the in-medium quark condensate. As we go away from the chiral limit in our pion cloud model, we adopt the same modification to the phenomenological nucleon correlator, and in doing so we need to make sure that there are no contributions to the OPE from the pion cloud that would violate the chiral counting rules to leading nonanalytic order. This is indeed the case, since the chiral expansion of the pion propagator contributes lowest order terms proportional to m_π^2 , maintaining the leading order behavior. Likewise, similar to the vacuum contribution illustrated in Figure 2a lowest dimension in-medium contributions shown in Figures 6a and 6b are possible. However, their effects are on higher order nonanalytic terms as they provide corrections proportional to ρm_π^3 and $\rho m_\pi^4 \ln(-m_\pi^2)$. Thus, to first order in baryon density the pion cloud model for the nucleon correlator in a nucleus is consistent with chiral perturbation theory in the leading nonanalytic contributions to the nucleon mass.

VI. RESULTS FOR THE NUCLEON MASS SHIFT IN SPIN-ISOSPIN SYMMETRIC NUCLEI

This model is best applied to light nuclei where there are large surface volume regions and therefore the density gradients extend over a large fraction of the nucleus. In infinite nuclear matter these density gradients are zero, so that the s-wave part of the πA optical potential, which we neglect dominates the in-medium pion cloud contribution to the nucleon correlator. In matter with $Z = N$, the strength of this potential is very small and the contributions of the diagrams in Figure 5 to the nucleon mass are negligible. As a result, the pion cloud has almost no effect on the nucleon mass in infinite nuclear matter, similar to the pion cloud effect on the nucleon mass in vacuum. It is evident that in large nuclei the pion cloud contribution to the nucleon mass becomes non-negligible only near the nuclear surface, a well-known property of the Kisslinger potential. So long as the nucleon remains a distance away from the surface comparable to about twice the πN interaction range (with $r_{\pi N} \sim 0.7$ fm) our mass shift result for this nucleon reproduce the work of previous authors [1,27]. Also application to large nuclei would require an extension of the method to account for $N \neq Z$.

In this paper, we work with models of two small symmetric nuclei that are familiar from πA scattering experiments, ^{16}O and ^{40}Ca . The nucleon density distribution of the ground states of both nuclei are given by Eq (3.16)). For ^{16}O we choose the parameters $c = 1.75$ fm and $\alpha = 2.0$ [32]. This produces a distribution of nucleons with a local minimum at $r = 0$ and an RMS radius of ~ 2.6 fm. The parameters for the ^{40}Ca density distribution are taken as $c = 2.80$ fm and $\alpha = 1.1$.

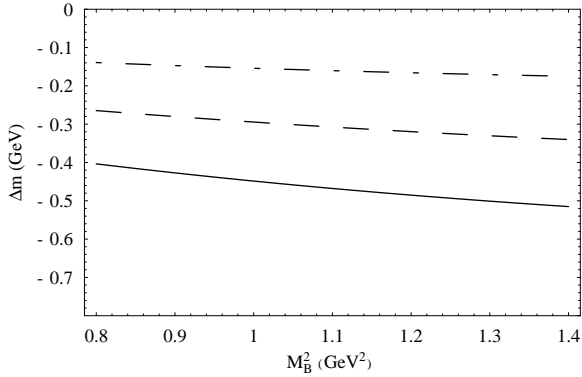


FIG. 7. The mass shifts in the ^{16}O nucleus at $0.5\rho_0$ with constant pion cloud probabilities. The solid line is the total mass shift, the dashed line is the mass shift due to the correlator without the pion cloud, and the dot-dashed line is the shift due to the pion cloud contribution.

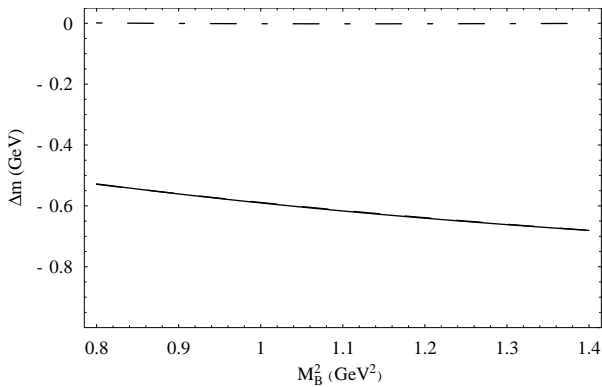


FIG. 8. The mass shifts in the ^{16}O nucleus at ρ_0 with constant pion cloud probabilities. The solid line is the total mass shift, the dashed line is the mass shift due to the correlator without the pion cloud, and the dot-dashed line is the shift due to the pion cloud contribution.

We find the mass shifts in the chiral limit, ignoring in our analysis the effects of the small leading nonanalytic terms discussed above. The mass shift of a nucleon in each nucleus is found by evaluating Eq. (5.12) in a Borel window

$0.8 \text{ GeV} \leq M_B^2 \leq 1.4 \text{ GeV}$. If the plot of the mass shift as a function of the Borel mass is relatively flat in this window, then the sum rules are sufficiently convergent and the mass shift is taken at this flat value. To test the stability of the sum rules we look at the mass shift at two points in the nucleus: first in the middle of the surface where the local density is half the nuclear matter density ρ_0 , then at the center of the nucleus, where the central density is equivalent to ρ_0 . As can be seen in Figures 7-10, the sum rules in both nuclei provide sufficiently stable solutions in the Borel window.

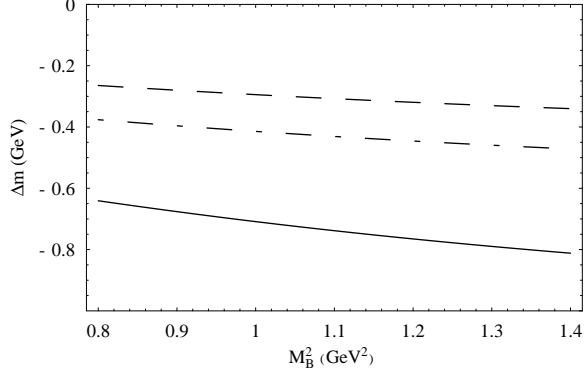


FIG. 9. The mass shifts in the ^{40}Ca nucleus at $0.5\rho_0$ with constant pion cloud probabilities. The solid line is the total mass shift, the dashed line is the mass shift due to the correlator without the pion cloud, and the dot-dashed line is the shift due to the pion cloud contribution.

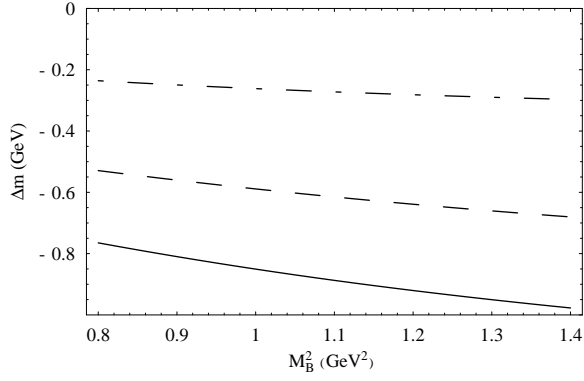


FIG. 10. The mass shifts in the ^{40}Ca nucleus at ρ_0 with constant pion cloud probabilities. The solid line is the total mass shift, the dashed line is the mass shift due to the correlator without the pion cloud, and the dot-dashed line is the shift due to the pion cloud contribution.

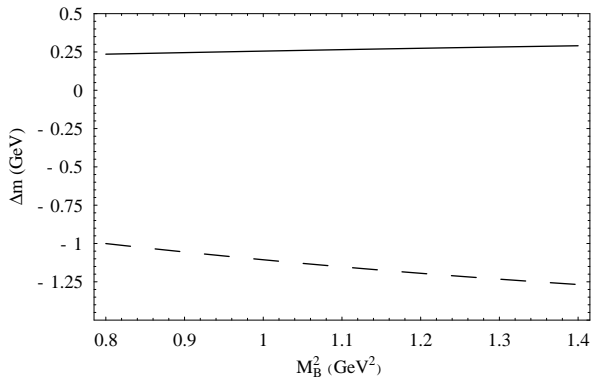


FIG. 11. The mass shift from the correlator structures in the ^{40}Ca nucleus at ρ_0 with constant pion cloud probabilities. The solid line is the mass shift from vector contributions to the correlator, and the dashed line is the mass shift due to scalar contributions to the correlator.

The convergence is amplified in the plots of the individual contributions of the vector and scalar correlators (Fig. 11). We find that the nucleon mass shift in an ^{16}O nucleus is negligible at the central baryon density, and -150 MeV at one-half central density. The mass shifts in a ^{40}Ca nucleus are -260 MeV at $\rho = \rho_0$ and -400 MeV at $\rho = \rho_0/2$.

Some pion cloud effects might be related to the spontaneous breaking of chiral symmetry. Since the reduction in the value the quark condensate is a signal of partial restoration of chiral symmetry in the nucleus, the pion cloud amplitude c_2 might decrease accordingly. We explore this idea by modifying our model, giving the pion cloud probability c_2^2 a linear dependence on density such that it has the vacuum value at zero density, and it vanishes at the density where the quark condensate $\langle \bar{q}q \rangle_\rho$ goes to zero. Similarly, the probability of no pion cloud c_1^2 increases from the vacuum value of 0.5 to the phase transition point value of 1.0. Figure 12 shows the mass shift of a nucleon in a ^{40}Ca nucleus at central density utilizing this modification to the model. The shift in ^{16}O shows a similar, if less dramatic, reduction. As in the constant pion cloud probability calculation, the sum rule calculation is sufficiently flat in the Borel window to provide a value for the mass shift. The mass shifts in ^{16}O are ~ 0 MeV at central and -100 MeV at surface density. In ^{40}Ca we find -100 MeV and -275 MeV, respectively.

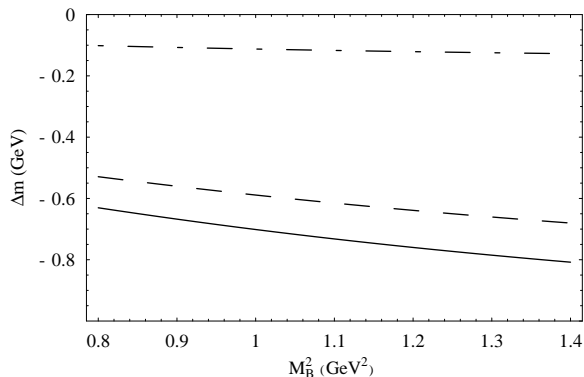


FIG. 12. The mass shifts in the ^{40}Ca nucleus at ρ_0 with pion cloud probabilities linearly scaling with density. The solid line is the total mass shift, the dashed line is the mass shift due to the correlator without the pion cloud, and the dot-dashed line is the shift due to the pion cloud contribution.

We compare these two methods to the sum rules without an explicit pion cloud throughout the nucleus in Figures 13 and 14. In these calculations, the density used at each point in the sum rules is the local density obtained from the density distribution (Eq. (3.16)) and the nucleon mass is plotted as a function of the distance from the center of the nucleus. Each mass shift is evaluated at the Borel mass $M_B = 1.0$ GeV.

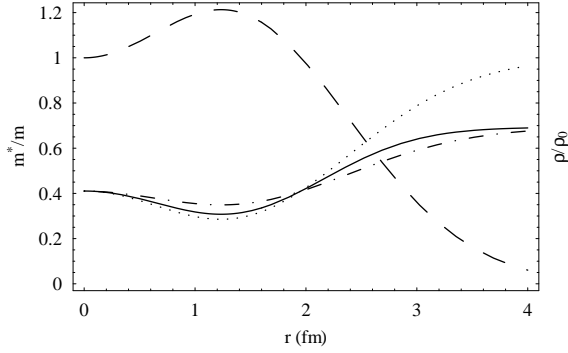


FIG. 13. The mass shifts in the ^{16}O nucleus as functions of distance from the nuclear center, calculated at a Borel mass of 1 GeV. The dashed line is the density distribution. The solid line is the nucleon mass with linearly scaling pion cloud probabilities, the dot-dashed line is the mass with constant probabilities, and the dotted line is the nucleon mass without the pion cloud contributions.

In an ^{16}O nucleus, the mass shift due to the pion cloud is small compared to the mass shift from the non-pionic terms but positive out to a distance of about 4.5 fm from the nuclear center. As the nucleon approaches the nuclear surface the pion cloud contribution to the mass shift becomes positive and larger than the mass shift without pion cloud. Even though the local density in the interval $3.0 \text{ fm} \leq r \leq 4.0 \text{ fm}$ is small (hence the small mass shift due to the correlator contributions without the pion cloud), the pion cloud is still sampling a significant range of density gradients leading to a sizable optical potential strength, and therefore a large mass shift. The two different approaches to the pion cloud amplitudes in ^{16}O do not yield significantly different results throughout the nucleus. In the ^{40}Ca nucleus, the mass shift due to the pion cloud is always negative and comparable to the non-pionic mass shift. As with the oxygen nucleus, the largest mass shift from the pionic terms occurs near the surface, approaching -600 MeV . The constant and linearly decreasing pion cloud probability calculations converge to the same value in this region. The nuclear interior shows a significant difference between the three methods. If c_1 and c_2 remain constant over the range of densities, then the pion cloud provides a rather large mass shift ($\sim -275 \text{ MeV}$ at central density). Once c_1 and c_2 are dependent on density, the pion cloud contribution is more than halved at the center of the nucleus, with a mass shift closer to -100 MeV . Clearly the choice of pion cloud method has a significant effect in larger nuclei.

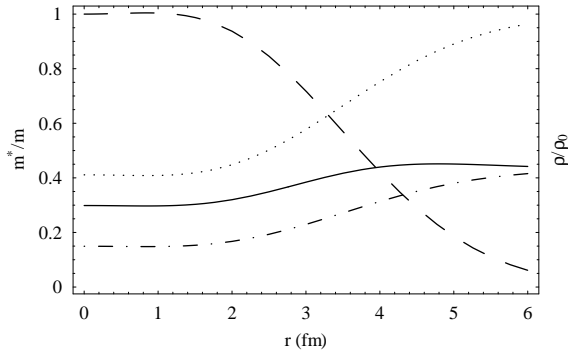


FIG. 14. The mass shifts in the ^{40}Ca nucleus as functions of distance from the nuclear center, calculated at a Borel mass of 1 GeV. The dashed line is the density distribution. The solid line is the nucleon mass with linearly scaling pion cloud probabilities, the dot-dashed line is the mass with constant probabilities, and the dotted line is the nucleon mass without the pion cloud contributions.

VII. CONCLUSIONS

We have described a model based on QCD for the nucleon in a finite spin and isospin symmetric nucleus including a pseudo-Goldstone boson component of the correlator. This approach is based on the model proposed by one of us in

Ref. [6], with the extension of the pion free propagator to the in-medium propagator using an optical potential which is first order in the nuclear density. A fit to chiral perturbation theory restricts the parameters of the pion cloud component. Our main conclusion is that there are significant contributions to the mass of the nucleon in the nucleus arising from the pion cloud component of the nucleon.

In the deep interior of the oxygen nucleus we find a small positive mass shift which becomes large and negative near the surface. In the calcium nucleus, however, the mass shift is everywhere large and negative. We introduce a parametrization of the pion cloud probability c_2^2 which decreases linearly from the vacuum value to zero at the chiral symmetry restoration as a possible test of partial restoration of chiral symmetry. At high densities, the effect of the pion cloud is then reduced leading to smaller mass shifts.

One obvious extension to this model is the consideration of the strange sector. By allowing for the inclusion of kaon cloud terms in the baryon current, we can construct similar sum rules for the mass shift of hyperons. The primary obstacles are the uncertainties of several in-medium matrix elements on the microscopic side, the complicated structure of the dispersion relation on the phenomenological side [24], and the difficulty in finding an appropriate form for the K - A optical potential to determine the kaon self-energy. The model can also be modified to handle $N \neq Z$ nuclei. The nucleon correlator in such nuclei without the pion cloud has been discussed in Ref. [1], and the optical potential is easily treated in asymmetric nuclei by including the isospin-dependent and spin flip terms in the πN scattering amplitude (Eq. (3.8)). A third venue of further research concerns the applications of the model to sea quark distributions in nuclei and the development of an improvement to QCD calculations of nuclear deep inelastic scattering in the interval $0.1 \leq x \leq 0.3$.

We would like to thank Mountaga Aw and Otto Linsuain for helpful discussions.

-
- [1] E. G. Drukarev and E. M. Levin, JETP Lett. **48**, 338 (1988); Sov. Phys. JETP **68**, 680 (1989); Nucl. Phys. **A511**, 679 (1990); Progr. Part. Nucl. Phys. **27**, 77 (1991).
 - [2] H. A. Bethe, Ann. Rev. Nucl. Sci. **21**, 125 (1971).
 - [3] J. D. Walecka, "Theoretical Nuclear and Subnuclear Physics" (Oxford University Press, New York) (1995).
 - [4] P. Langacker and H. Pagels, Phys. Rev. **D8**, 4595 (1973).
 - [5] J. Gasser and H. Leutwyler, Ann. Phys. **158**, 142 (1984).
 - [6] L. S. Kisslinger, [hep-th/9811497](#).
 - [7] P. Amadruz, et. al., Phys. Rev. Lett. **66**, 2717 (1991);
M. Arnedo, et.al., Phys. Rev **D50**, R1 (1994).
 - [8] E. A. Hawker, et. al., Phys. Rev. Lett. **80**, 3715 (1998) ;
J. C. Peng, et. al., Phys. Rev. **D56**, 92004 (1998).
 - [9] D. A. Ross and C. T. Sachrajda, Nucl. Phys. **B149**, 497 (1979).
 - [10] H. Jung and L. S. Kisslinger, Nucl. Phys. **A586**, 682 (1995).
 - [11] J. D. Sullivan, Phys. Rev. **D5**, 1732 (1972).
 - [12] J. Speth and A. W. Thomas, Adv. Nucl. Phys. **24**, 83 (1998).
 - [13] P. L. McGaughey, J. M. Moss and J. C. Peng, Ann. Rev. Nucl. Part. Sci. **49**, 217 (1999).
 - [14] J. Gasser and A. Zepeda, Nucl. Phys. **B174**, 445 (1980).
 - [15] S. H. Lee, S. Choe, T. D. Cohen, and D. K. Griegel, Phys. Lett. **B348**, 263 (1995).
 - [16] M. C. Birse, Phys. Rev. **C 53**, R2048 (1996);
M. C. Birse and B. Krippa, Phys. Lett. **B 381**, 397 (1996).
 - [17] B. L. Ioffe, Nucl. Phys. **B188**, 317 (1981); **B191**, 591 (E) (1981);
V. M. Belayev and B. L. Ioffe, Sov. Phys. JETP **56**, 493 (1982).
 - [18] L. S. Kisslinger and Z. Li, Phys. Rev. Lett. **74**, 2168 (1995).
 - [19] B. L. Ioffe and A. V. Smilga, Nucl. Phys. **B232**, 109 (1984).
 - [20] J. M. Eisenberg and D. S. Koltun, "Theory of Meson Interactions with Nuclei" (John Wiley and Sons, New York) (1979).
 - [21] L. S. Kisslinger, Phys. Rev. **98**, 761 (1955).
 - [22] T. D. Cohen, R. J. Furnstahl, and D. K. Griegel, Phys. Rev. Lett. **67**, 961 (1991); Phys. Rev. **C46**, 1507 (1992);
T. D. Cohen, R. J. Furnstahl, D. K. Griegel, and X. Jin, Phys. Rev. **C47**, 2882 (1993);
T. D. Cohen, R. J. Furnstahl, D. K. Griegel, X. Jin, and M. Nielsen, Phys. Rev. **C49**, 464 (1994).
 - [23] J. Gasser and H. Leutwyler, Phys. Reports **87**, 77 (1982).
 - [24] E. M. Henley and J. Pasupathy, Nucl. Phys. **A556**, 467 (1992).
 - [25] T. P. Cheng, Phys. Rev. **D38**, 2869 (1988);

- J. Gasser, M. E. Sainio, and A. Svarc, Nucl. Phys. **B307**, 779 (1988).
- [26] M. B. Johnson and L. S. Kisslinger, Phys. Rev. **C52**, 1022 (1995).
 - [27] E. G. Drukarev and M. G. Ryskin, Nucl. Phys. **A578**, 333 (1994); Z. Phys. **A356**, 457 (1997).
 - [28] V. L. Eletsky, Phys. Lett. **B245**, 229 (1990).
 - [29] Y. Koike, Phys. Rev. **D48**, 2313 (1993).
 - [30] S. Weinberg, Phys. Lett. **251**, 288 (1990); Nucl.Phys. **B363**, 1 (1991); Phys. Lett. **B295**, 114 (1992).
 - [31] T. P. Cheng and L. F. Li, “Gauge Theory of Elementary Particle Physics” (Clarendon Press, Oxford) (1992)
 - [32] H. De Vries, C. W. De Jager, and C. De Vries, At. Data Nucl. Data Tables **36**, 495 (1987);
M. B. Johnson and G. R. Satchler, Ann. Phys. (N.Y.) **248**, 134 (1996).